[redacted]

Copy
RM E55B28





# RESEARCH MEMORANDUM

## INVESTIGATION OF A HIGH-PRESSURE-RATIO EIGHT-STAGE AXIAL-FLOW RESEARCH COMPRESSOR WITH TWO TRANSONIC INLET STAGES

## IV - MODIFICATION OF AERODYNAMIC DESIGN AND PREDICTION OF PERFORMANCE

By Richard P. Geye and Charles H. Voit

Lewis Flight Propulsion Laboratory
Cleveland, Ohio







NATIONAL ADVISORY COMMITTEE
FOR AERONAUTICS

WASHINGTON

June 1, 1955

[redacted]

[redacted]

NATIONAL ADVISORY COMMITTEE FOR AERONAUTICS

RESEARCH MEMORANDUM

# INVESTIGATION OF A HIGH-PRESSURE-RATIO EIGHT-STAGE AXIAL-FLOW RESEARCH COMPRESSOR WITH TWO TRANSONIC INLET STAGES

## IV - MODIFICATION OF AERODYNAMIC DESIGN AND PREDICTION OF PERFORMANCE

By Richard P. Geye and Charles H. Voit



## SUMMARY

An eight-stage high-pressure-ratio axial-flow compressor, designed for use as a research compressor, was modified to improve design-speed performance and to provide an instrument for continued study of the problems associated with design and off-design performance of transonic stages combined with highly loaded subsonic stages. This compressor consisted of two transonic inlet stages and six subsonic stages modified to produce a maximum design-speed over-all total-pressure ratio of 10.90 at an equivalent weight flow of 30.0 pounds per square foot of rotor frontal area. The compressor tip diameter was increased from 20 to 20.86 inches at the compressor inlet and decreased linearly to the original 20-inch diameter at the inlet to the seventh stage. The increase in the inlet tip diameter resulted in a first-stage design tip speed of 1218 feet per second, a maximum relative tip Mach number of 1.25, and an inlet hub-tip ratio of 0.46.

This report also discusses the method used for predicting the performance of the modified compressor and compares the results of this prediction with the over-all performance of the original compressor.

## INTRODUCTION

The use of transonic inlet stages in an axial-flow compressor presents a means by which weight flow per unit frontal area, or average stage pressure ratio, or both, can be increased. In order to study the problems associated with staging transonic inlet stages with highly loaded subsonic stages, the eight-stage compressor of reference 1 was built and operated as a research unit.

The results of the investigation of this compressor (ref. 2) show that, at design speed, a maximum over-all pressure ratio of approximately

[redacted]

9.90, a maximum average stage pressure ratio of approximately 1.33, and an adiabatic temperature-rise efficiency of 0.82 were attained at an equivalent weight flow of 29.6 pounds per square foot of frontal area. It is apparent that the design-speed weight flow and the stage loadings of this compressor are higher than those employed in most current commercial designs; however, the design-speed over-all pressure ratio and efficiency did not attain the values anticipated by the design calculations (ref. 1).

The blade angles of several of the stator rows were reset in an attempt to improve the design-speed performance, and the investigation of the compressor was continued. During this phase of the investigation, a fatigue failure in one or more of the blade rows resulted in complete destruction of all compressor blading. In order to provide a research unit for continued study of the effects of high blade loading and high over-all pressure ratio along with the performance of transonic stages, the compressor blading was refabricated. Furthermore, in an attempt to remedy as far as practicable the mechanical and aerodynamic deficiencies of the compressor as originally designed, simple modifications intended to improve the fatigue strength of the blades and to increase the design-speed over-all pressure ratio and efficiency were incorporated in the compressor reblading design.



The present report discusses the modifications made in rebuilding the compressor and outlines the procedure used for predicting the performance of the modified compressor. The predicted performance characteristics are presented and compared with the performance characteristics of the compressor of reference 1.

## DESIGN MODIFICATIONS

Three deficiencies became apparent during the over-all and interstage performance investigations of the compressor of reference 1: (1) The design over-all pressure ratio and efficiency were not attained; (2) the performance of the second stage was poorer than anticipated; and (3) the fatigue strength of the blades was less than required to withstand the stresses encountered during certain phases of compressor operation. Design modifications were incorporated in the rebuilding of the compressor to overcome these deficiencies.

### Rematching of Stages

From the information available on over-all compressor performance and individual stage performance in references 2 and 3, it is apparent that the original compressor design incorporated too large an allowance for boundary-layer growth through the compressor (ref. 1). As a

result, at design speed the axial velocities through the compressor decreased at a rate greater than anticipated, and the rear stages stalled while the front stages were still operating at low angles of incidence. Because of this, the front stages operated below their design pressure ratios and efficiencies at design speed, and the compressor did not attain its design over-all pressure ratio and efficiency. (Flow coefficients at the design-speed maximum pressure ratio for the compressor of ref. 1 are presented in fig. 1 to indicate the performance of the stages at this point.)



Hence, to increase the over-all compressor pressure ratio and efficiency at design speed, an adjustment in stage matching is necessary. In order to avoid an elaborate change in the aerodynamic configuration of the compressor blading so that existing blade masters can be used, stage matching will be adjusted by changing the annulus-area (axial-velocity) variation through the compressor. Because of the physical limitations imposed by the internal and external dimensions of the existing compressor casing, it is not possible to completely rematch the stages so that they will all operate at their design pressure ratios simultaneously.

Change in casing contour. - To attain the improvement in matching that is possible within the limits of the casing dimensions, the internal casing diameter at the entrance of the seventh stage (station 7, fig. 2) was held at 20.00 inches, and the diameter at the entrance of the first stage (station 1, fig. 2) was increased to 20.86 inches. From the entrance of the first stage to the entrance of the seventh stage, the internal casing diameter was decreased linearly from 20.86 to 20.00 inches. (The region of this change in casing contour is indicated in fig. 2.)

Change in hub curvature. - It was felt that the poor performance of the second stage (ref. 3) might have been caused by a mismatching of the various blade elements due to a maldistribution of the axial velocity caused by the large change in hub curvature preceding this stage. The importance of such curvature effects is indicated in reference 4. In order to reduce the magnitude of the effect which hub-curvature might have on the second-stage performance, the rate of change of hub curvature through the first and second stages was reduced to the minimum that was compatible with strength requirements in the second-stage rotor disk. (The location of this change in hub curvature is indicated in fig. 2.)

With the new annulus areas obtained with the modified casing and hub contours, the stage flow coefficients were determined for a design-speed over-all pressure ratio of 10.26 (the design pressure ratio of the original compressor, ref. 1) by using the stage-stacking method presented in appendix B. (Symbols are defined in appendix A.) Comparison of these flow coefficients with those obtained at the maximum design-speed pressure ratio of the original compressor (fig. 1) reveals that, with the

new annulus-area variation, the front stages operate at lower flow coefficients (higher angles of incidence) and the rear stages operate at higher flow coefficients (lower angles of incidence). As a result of this improved stage matching, the over-all compressor performance characteristics should be improved at design speed.

### Blade Modifications

The aerodynamic configuration of the compressor blading is the same as that used in the compressor of reference 1, except that (1) blade twist, thickness, and camber variations were extrapolated to facilitate lengthening the blades as required by the increase in the flow passage area from the first through the sixth stages, and (2) blade base fillets were enlarged to reduce the possibility of blade failure during the investigation of certain modes of compressor operation in which high vibrational stresses are encountered. A 0.06-inch-radius fillet was used in each blade row of the original compressor design. These fillets were enlarged to 0.12-inch-radii in the blade rows of the last five stages and to 0.18-inch-radii faired hyperbolically into the blade contour 0.5 inch up from the blade base in the blade rows of the first three stages.

3582

## PREDICTION OF MODIFIED-COMPRESSOR PERFORMANCE

### Calculation of Over-All Performance

The stage performance characteristics (ref. 3) of the compressor of reference 1 are presented in figure 1, with stage equivalent total-pressure ratio and stage equivalent temperature-rise ratio plotted as functions of flow coefficient. These stage characteristics, together with the values of area ratio, radius ratio, design temperature ratio (ref. 1), and absolute air angle (ref. 1) presented in table I, were used in calculating the over-all performance by the method presented in appendix B.

In thus calculating the over-all performance, the following assumptions are implied: (1) The absolute air angles leaving the stators remain constant over the entire range of compressor operation; (2) the effects of compressibility and Reynolds number on stage efficiency and flow range can be neglected except in the eighth stage, where the flow range of the stage data (ref. 3) is great enough to indicate these effects; (3) an increase in flow passage area at the entrance to a stage will not result in a basic change in the average stage performance characteristics but will serve only to decrease the stage flow coefficient for a given equivalent weight flow and wheel speed; (4) the extension of blade lengths as required by the increases in flow passage area will not affect

the average stage performance at a given flow coefficient; (5) boundary layer thickness through the compressor will not be altered by flow passage modifications; and (6) the increase in fillet size will not result in an appreciable change in average stage performance, although the over-all compressor efficiency will probably be decreased by the use of large-base fillets (ref. 5).

Using the method presented in appendix B, a number of over-all compressor performance points were calculated at 30, 50, 60, 70, 80, 90, and 100 percent of equivalent design speed and the compressor performance characteristics at these various speeds were determined.



## Approximation of Compressor Surge-Limit Line

When the calculated stage flow coefficients of the modified compressor were approximately equal to the corresponding stage flow coefficients obtained at a surge point for the compressor of reference 1, the modified compressor was assumed to surge.

In order to illustrate the manner in which a point on the modified compressor surge-limit line was determined under this assumption, an example is presented in figure 3. In this example, a point was chosen on the surge-limit line of the compressor of reference 1 at which the flow coefficient for each stage was known (the surge point at 80 percent of design speed). The value of the first-stage flow coefficient was obtained from figure 4(a) of reference 3, and the path along which this flow coefficient can be maintained was superimposed on the modified compressor performance map in figure 3. A similar procedure was followed for each of the other seven stages.

Thus, each line superimposed on the performance map in figure 3 represents a path of constant flow coefficient for one of the stages in the modified compressor. It is apparent that these paths converge and cross at a common point. (These paths probably would not converge to such a well defined point if the area modification through the compressor were large or irregular.) At the point of intersection, all eight stages of the modified compressor have calculated flow coefficients approximately equal to the corresponding stage flow coefficients found at a surge point of the compressor of reference 1; therefore, this point was assumed to lie on the surge-limit line of the modified compressor. As would be expected in view of the area modifications made in the compressor, the point of convergence occurred at a higher equivalent speed in the modified compressor than in the compressor of reference 1. Consequently, there was a Mach number effect which would tend to displace the predicted surge-limit point from that which will actually be attained; however, since the equivalent-speed change was not large, the magnitude of this effect will probably be small, and the surge point as predicted is assumed to be a reasonable approximation.

Using the values of stage flow coefficients obtained at surge points at 30, 50, 60, 70, 90, and 100 percent of equivalent design speed for the compressor of reference 1, a similar procedure was followed and the corresponding modified-compressor surge points were determined. A line faired through these points was taken to represent the modified-compressor surge limit (fig. 4).

## RESULTS

### Design Point Characteristics

The various compressor characteristics determined for the compressor design point in the design modification procedure are as follows (values given are for standard sea-level inlet conditions):

| | |
|---|---|
| Over-all total-pressure ratio | 10.26 |
| Weight flow per unit rotor frontal area, (lb/sec)/sq ft | 30.5 |
| Wheel speed, rpm | 13,380 |
| Over-all adiabatic efficiency | 0.86 |

### Predicted Changes in Compressor Performance

The calculated over-all performance characteristics of the modified compressor and the actual over-all performance characteristics of the compressor of reference 1 are compared in figures 4 and 5, where total-pressure ratio and adiabatic temperature-rise efficiency, respectively, are plotted against equivalent weight flow per unit frontal area over a range of equivalent speeds from 30 to 100 percent of design.

The changes in compressor performance which should result from the design modifications incorporated are apparent. Design-speed performance should be improved. The maximum pressure ratio at design speed should be increased from 9.90 to 10.90, the maximum weight flow per unit frontal area from 29.6 to 30.7 pounds per second, and the peak efficiency from 82 to 87 percent. However, with these improvements in design-speed performance, part-speed performance should be adversely affected. The equivalent speed at which the knee in the surge line is encounted in the modified compressor should be increased from 63 to approximately 72 percent of design speed, and the area of rotating stall should be increased by a similar speed increment. In addition, the compressor modifications should result in a decrease in the weight flow per unit frontal area and the peak efficiencies attainable below 90 percent of equivalent design speed (fig. 5).

Lewis Flight Propulsion Laboratory
National Advisory Committee for Aeronautics
Cleveland, Ohio, March 23, 1955

[redacted]

## APPENDIX A

## SYMBOLS

The following symbols are used in this report:

| | |
|---|---|
| $A$ | annulus area, sq ft |
| $c_p$ | specific heat at constant pressure, Btu/(lb)($^\circ$F) |
| $g$ | acceleration due to gravity, 32.174 ft/sec$^2$ |
| $J$ | mechanical equivalent of heat, 778 ft-lb/Btu |
| $P$ | total pressure, lb/sq ft |
| $R$ | gas constant, ft-lb/(lb)($^\circ$F) |
| $r$ | radius, ft |
| $T$ | total temperature, $^\circ$R |
| $U$ | wheel speed, ft/sec |
| $V$ | velocity, ft/sec |
| $W$ | weight-flow rate, lb/sec |
| $W\sqrt{\theta}/\delta$ | equivalent weight flow, lb/sec |
| $\beta$ | flow angle measured from the axial direction, deg |
| $\gamma$ | ratio of specific heats |
| $\delta$ | ratio of total pressure to NACA standard sea-level pressure of 2116 lb/sq ft |
| $\eta$ | adiabatic temperature-rise efficiency |
| $\theta$ | ratio of total temperature to NACA standard sea-level temperature of 518.7$^\circ$ R |
| $\rho$ | density, lb-sec$^2$/ft$^4$ |
| $\varphi$ | flow coefficient, $(V_a/U)_m$ |

[redacted]

Subscripts:

| | |
|---|---|
| a | axial |
| d | design conditions |
| e | equivalent, indicates that parameter to which it is affixed has been corrected for speed |
| m | mean radius |
| n | station |
| s | static |
| 0 | standard sea-level conditions |
| t | total |
| 1 | compressor-inlet station |
| 2,3, . . ., 9 | stations at exit of first, second, . . ., eighth stages |



[redacted]

## APPENDIX B

## CALCULATIONS OF PERFORMANCE OF MODIFIED EIGHT-STAGE AXIAL-FLOW COMPRESSOR

In order to obtain an indication of the effect of the design changes on design and off-design compressor performance, a one-dimensional technique of stage stacking (ref. 6) was used to predict the over-all performance characteristics of the modified eight-stage compressor from the stage performance curves of the original compressor (ref. 3).

For simplicity of calculation, the individual stage data for all speeds are correlated on the basis of equivalent total-pressure ratio $(P_{n+1}/P_n)_e$ and equivalent temperature-rise ratio $(\Delta T/T_n)_e$ as plotted against flow coefficient $\varphi$. The flow coefficient is defined as follows:

$$\varphi = \left(\frac{V_a}{U}\right)_m \tag{B1}$$

The equivalent performance parameters (developed in ref. 7) are defined as follows:

$$\left(\frac{P_{n+1}}{P_n}\right)_e = \left\{\left[\left(\frac{P_{n+1}}{P_n}\right)^{\frac{\gamma-1}{\gamma}} - 1\right]\frac{\left(\frac{U}{\sqrt{T_n}}\right)_d^2}{\left(\frac{U}{\sqrt{T_n}}\right)^2} + 1\right\}^{\frac{\gamma}{\gamma-1}} \tag{B2}$$

$$\left(\frac{\Delta T}{T_n}\right)_e = \left(\frac{\Delta T}{T_n}\right)\frac{\left(\frac{U}{\sqrt{T_n}}\right)_d^2}{\left(\frac{U}{\sqrt{T_n}}\right)^2} \tag{B3}$$

The flow coefficient into the first stage is determined from the conventional weight-flow parameter $W\sqrt{\theta_1}/\delta_1$, the rotative speed $U_{m,1}/\sqrt{\theta_1}$, and the effective stage-inlet area.

From continuity,

$$V_{a,1} = \frac{W}{g\rho_{s,1}A_1}$$

or

$$\frac{V_{a,1}}{\sqrt{\theta_1}} = \frac{W\sqrt{\theta_1}T_0P_1}{\delta_1 A_1 T_1 P_0 g\rho_{s,1}} \tag{B4}$$

By combining equation (B4) with the perfect gas law

$$\frac{P_1}{T_1} = gR\rho_{t,1} \tag{B5}$$

with the expression

$$\frac{\rho_{s,1}}{\rho_{t,1}} = \left(1 - \frac{V_1^2}{2gJc_pT_1}\right)^{\frac{1}{\gamma-1}} \tag{B6}$$

and with the vector-diagram relation

$$V_1 = \frac{V_{a,1}}{\cos \beta_1} \tag{B7}$$

the following equation is obtained:

$$\frac{W\sqrt{\theta_1}}{\delta_1 A_1} = \frac{V_{a,1}}{\sqrt{\theta_1}}\left[1 - \left(\frac{V_{a,1}}{\sqrt{\theta_1}}\right)^2 \frac{1}{2gJc_pT_0 \cos^2 \beta_1}\right]^{\frac{1}{\gamma-1}} g\rho_0 \tag{B8}$$

With an estimated value of $W\sqrt{\theta_1}/\delta_1 A_1$ and the value of $\beta_1$ given in table I, equation (B8) can be solved and a value of $V_{a,1}/\sqrt{\theta_1}$ obtained. The flow coefficient is then determined from the equation

$$\varphi_1 = \frac{\frac{V_{a,1}}{\sqrt{\theta_1}}}{\frac{U_{m,1}}{\sqrt{\theta_1}}} \tag{B9}$$

After the flow coefficient has been determined, the values of equivalent total-pressure ratio and equivalent temperature-rise ratio are obtained from the generalized stage-performance curves (fig. 1). The stage pressure ratio is obtained from the equivalent total-pressure ratio as follows:



[redacted]

$$\frac{P_2}{P_1} = \left\{ \left[ \left( \frac{P_2}{P_1} \right)_e^{\frac{\gamma-1}{\gamma}} - 1 \right] \frac{\left( \frac{U}{\sqrt{T_1}} \right)^2}{\left( \frac{U}{\sqrt{T_1}} \right)_d^2} + 1 \right\}^{\frac{\gamma}{\gamma-1}} \tag{B10}$$

and the stage temperature ratio, from the equivalent temperature-rise ratio:

$$\frac{T_2}{T_1} = 1 + \left( \frac{\Delta T_{1-2}}{T_1} \right)_e \frac{\left( \frac{U}{\sqrt{T_1}} \right)^2}{\left( \frac{U}{\sqrt{T_1}} \right)_d^2} \tag{B11}$$

The weight-flow parameter for the second stage $W\sqrt{\theta_2}/\delta_2 A_2$ is determined from the parameter for stage 1, the values of $P_2/P_1$ and $T_2/T_1$ determined from equations (B10) and (B11), and the value of $A_1/A_2$ presented in table I, by using the expression

$$\frac{W\sqrt{\theta_2}}{\delta_2 A_2} = \frac{W\sqrt{\theta_1}}{\delta_1 A_1} \frac{A_1}{A_2} \frac{\sqrt{T_2/T_1}}{P_2/P_1} \tag{B12}$$

The rotative speed $U_{m,2}/\sqrt{\theta_2}$ is determined from the rotative speed of the first stage, from $T_2/T_1$, which was obtained from equation (B11), and from $r_2/r_1$, which is presented in table I, by the following equation:

$$\frac{U_{m,2}}{\sqrt{\theta_2}} = \frac{U_{m,1}}{\sqrt{\theta_1}} \frac{(r_2/r_1)}{\sqrt{T_2/T_1}} \tag{B13}$$

With the value of $W\sqrt{\theta_2}/\delta_2 A_2$ determined from equation (B12) and $\beta_2$ given in table I, a value of $V_{a,2}/\sqrt{\theta_2}$ can be determined by using equation (B8). Then the flow coefficient at the entrance to the second stage, $\varphi_2$, can be found:

$$\varphi_2 = \frac{\frac{V_{a,2}}{\sqrt{\theta_2}}}{\frac{U_{m,2}}{\sqrt{\theta_2}}}$$

[redacted]

After the flow coefficient has been determined, the values of equivalent total-pressure ratio and temperature-rise ratio for the second stage can be obtained from figure 1, and the actual pressure ratio and temperature for this stage can be computed in a manner similar to that outlined for the first stage. This process is repeated for each stage throughout the compressor. Over-all pressure ratio and temperature ratio are taken as the products of the stage values, and the over-all adiabatic efficiency is computed from over-all temperatures and pressures. For all performance calculations, inlet weight flows must be properly chosen so that all stages remain within the limits of their individual flow ranges.

3582

## REFERENCES

1. Voit, Charles H.: Investigation of a High-Pressure-Ratio Eight-Stage Axial-Flow Research Compressor with Two Transonic Inlet Stages. I - Aerodynamic Design. NACA RM E53I24, 1953.

2. Geye, Richard P., Budinger, Ray E., and Voit, Charles H.: Investigation of a High-Pressure-Ratio Eight-Stage Axial-Flow Research Compressor with Two Transonic Inlet Stages. II - Preliminary Analysis of Over-All Performance. NACA RM E53J06, 1953.

3. Voit, Charles H., and Geye, Richard P.: Investigation of a High-Pressure-Ratio Eight-Stage Axial-Flow Research Compressor with Two Transonic Inlet Stages. III - Individual Stage Performance Characteristics. NACA RM E54H17, 1954.

4. Hatch, James H., Giamati, Charles C., and Jackson, Robert J.: Application of Radial-Equilibrium Condition to Axial Flow Turbomachine Design Including Consideration of Change of Entropy with Radius Downstream of Blade Row. NACA RM E54A20, 1954.

5. King, J. Austin, and Regan, Owen W.: Performance of NACA Eight-Stage Axial-Flow Compressor at Simulated Altitudes. NACA WR E-5, 1944. (Supersedes NACA ACR E4L21.)

6. Benser, William A.: Analysis of Part-Speed Operation for High-Pressure-Ratio Multistage Axial-Flow Compressors. NACA RM E53I15, 1953.

7. Medeiros, Arthur A., Benser, William A., and Hatch, James E.: Analysis of Off-Design Performance of a 16-Stage Axial-Flow Compressor with Various Blade Modifications. NACA RM E52L03, 1953.

[redacted]

TABLE I. - DESIGN DATA

| Station | Annulus-area ratio, $A_{n-1}/A_n$ | Mean radius ratio, $r_n/r_{n-1}$ | Design total-temperature ratio, $T_n/T_{n-1}$ | Absolute air angle at mean radius, $\beta_n$, deg |
|---|---|---|---|---|
| 1 | | | | 0 |
| 2 | 1.222 | 1.088 | 1.108 | 16.82 |
| 3 | 1.189 | 1.043 | 1.108 | 29.65 |
| 4 | 1.189 | 1.034 | 1.083 | 29.61 |
| 5 | 1.208 | 1.028 | 1.091 | 29.52 |
| 6 | 1.242 | 1.024 | 1.096 | 28.72 |
| 7 | 1.246 | 1.018 | 1.098 | 26.86 |
| 8 | 1.207 | 1.013 | 1.095 | 27.24 |
| 9 | | | 1.091 | |

[redacted]

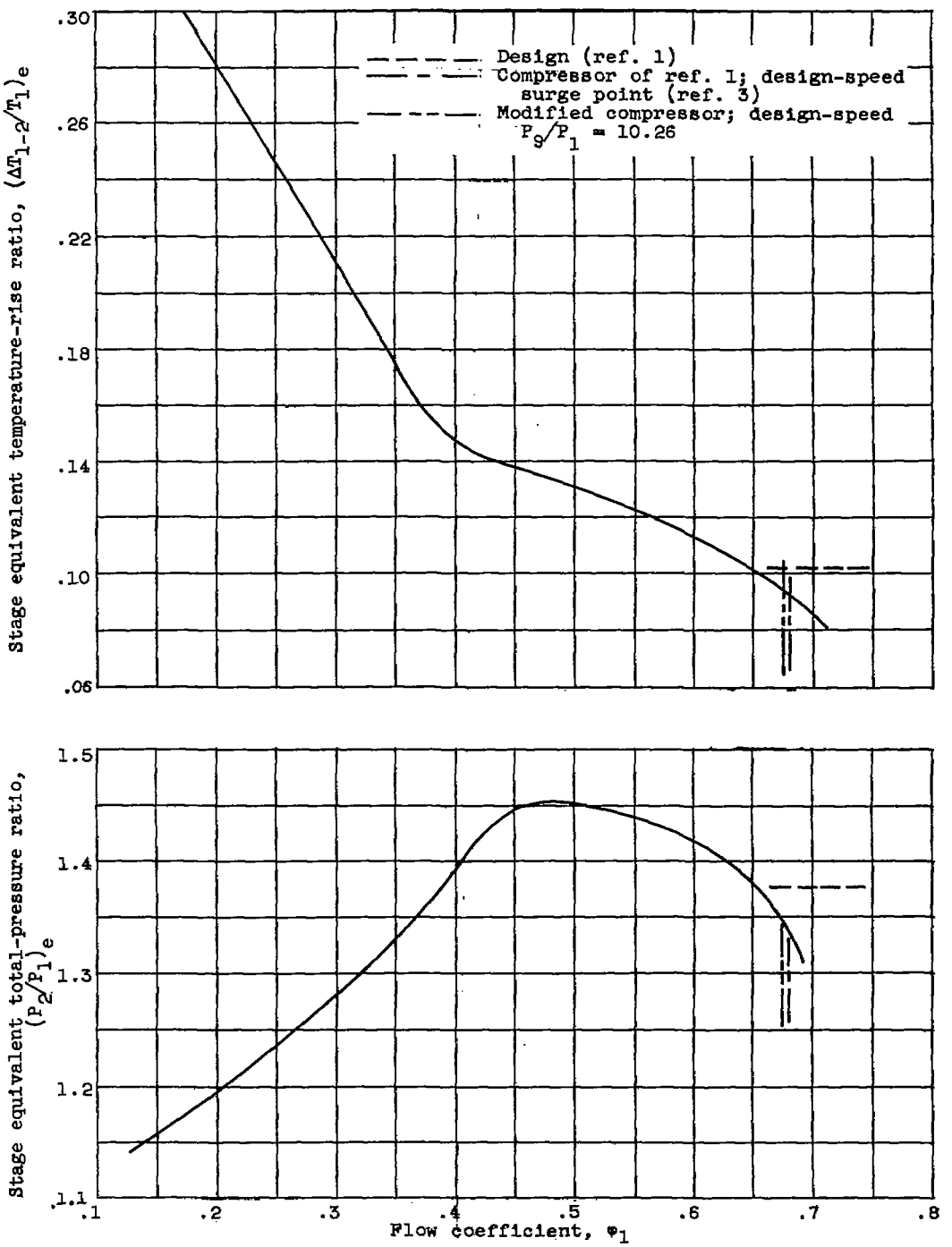


(a) First stage.

Figure 1. - Individual stage performance of eight-stage compressor over entire flow range. Speeds, 30 to 100 percent of equivalent design speed.

[redacted]

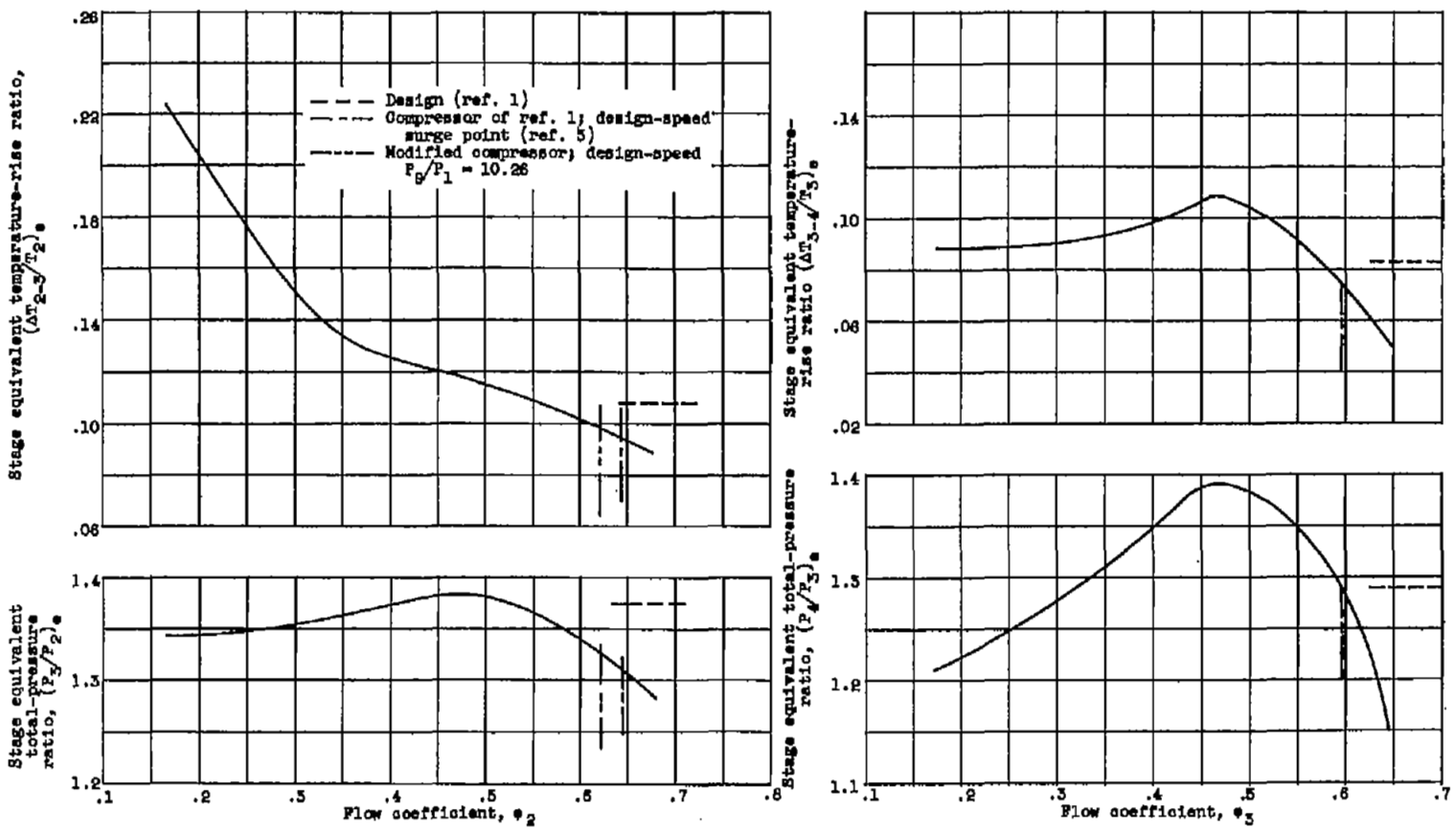


(b) Second stage.

(c) Third stage.

Figure 1. - Continued. Individual stage performance of eight-stage compressor over entire flow range. Speeds, 30 to 100 percent of equivalent design speed.

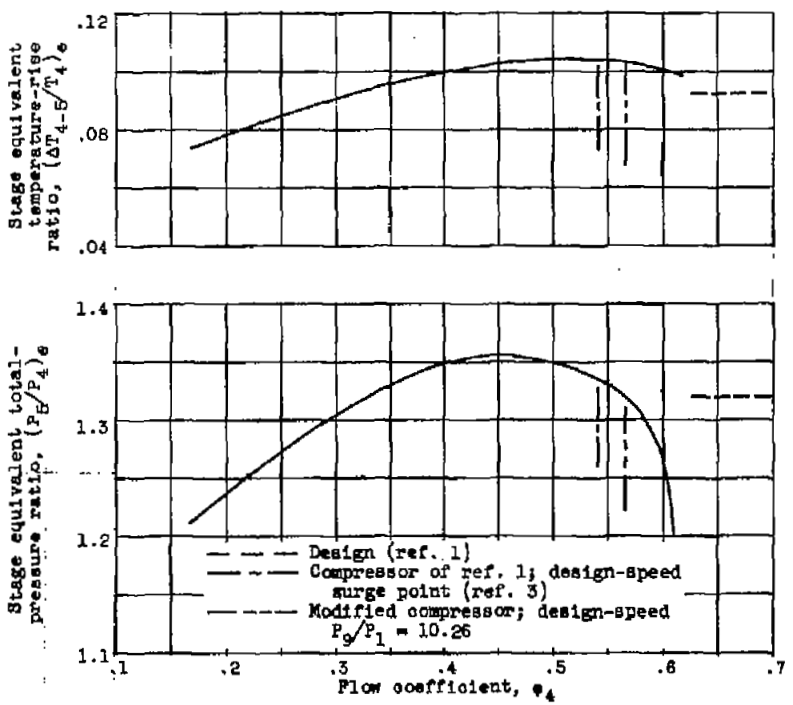


(d) Fourth stage.

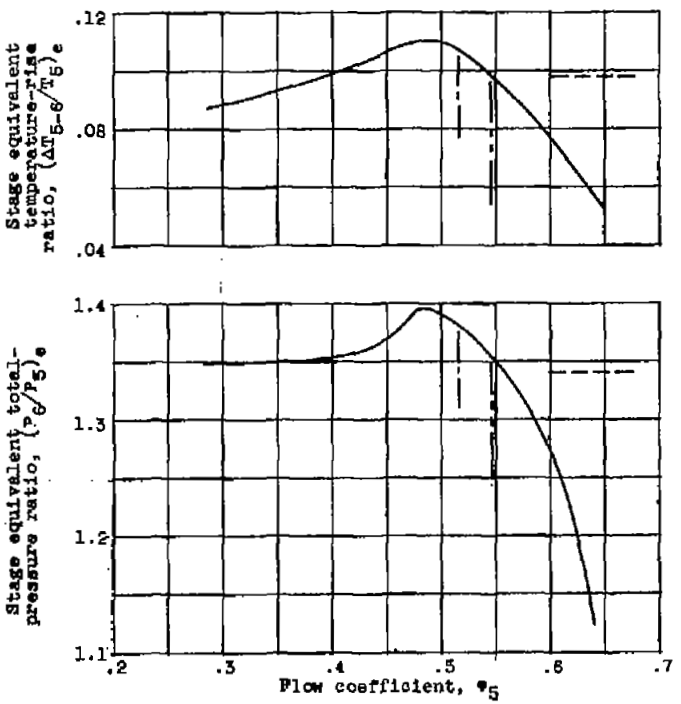


(e) Fifth stage.

Figure 1. - Continued. Individual stage performance of eight-stage compressor over entire flow range. Speeds, 30 to 100 percent of equivalent design speed.

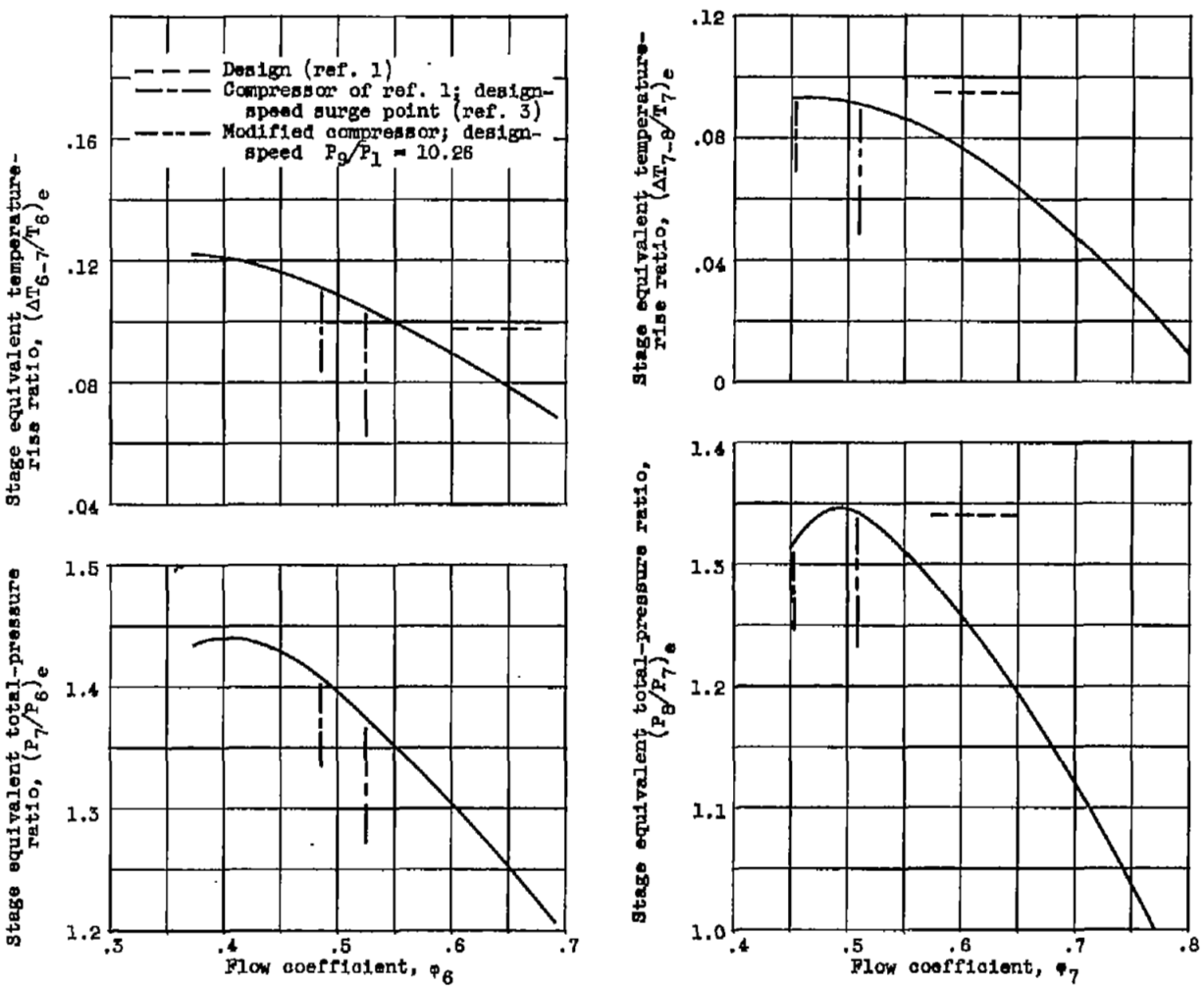


(f) Sixth stage.

(g) Seventh stage.

Figure 1. - Continued. Individual stage performance of eight-stage compressor over entire flow range. Speeds, 30 to 100 percent of equivalent design speed.

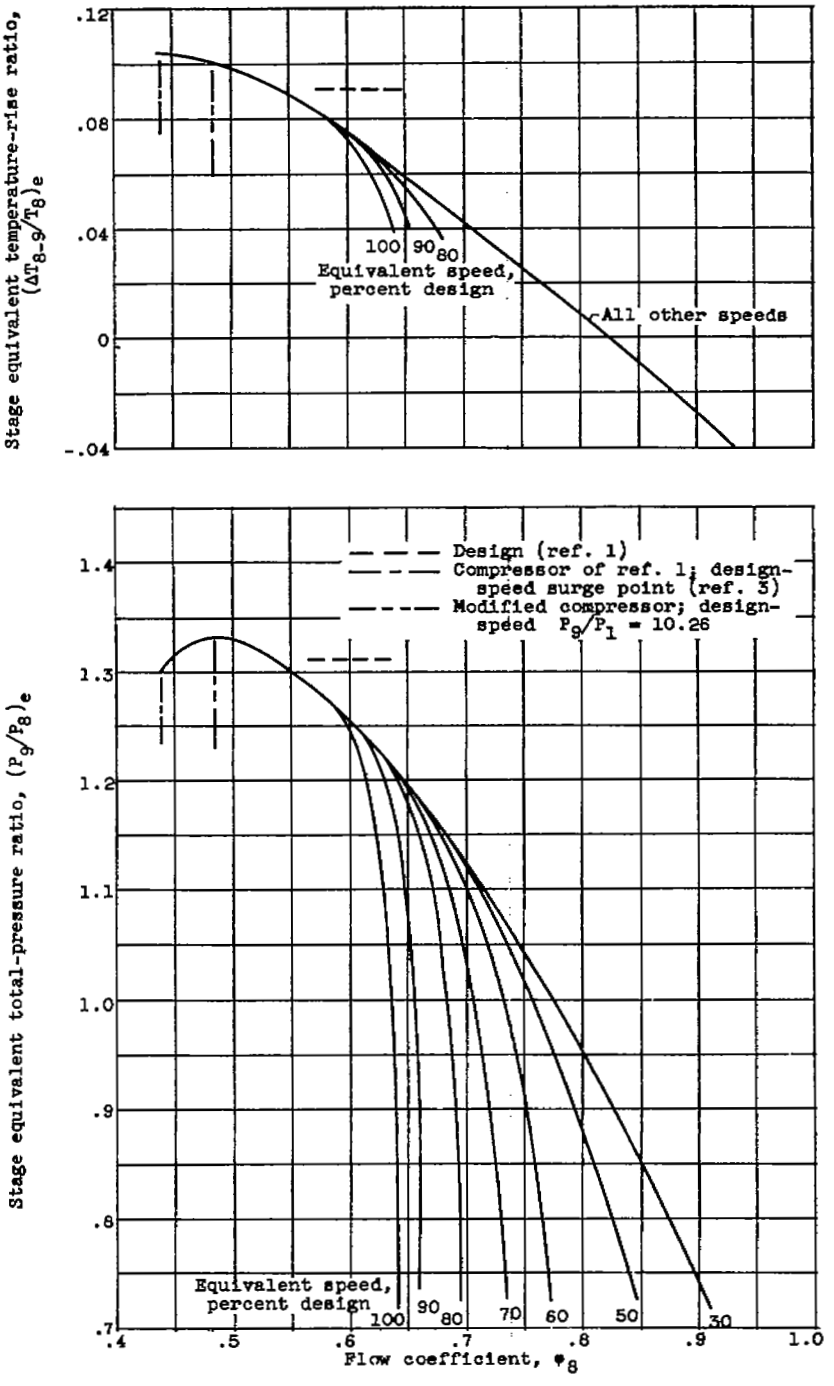


(h) Eighth stage.

Figure 1. - Concluded. Individual stage performance of eight-stage compressor over entire flow range. Speeds, 30 to 100 percent of equivalent design speed.

[redacted]

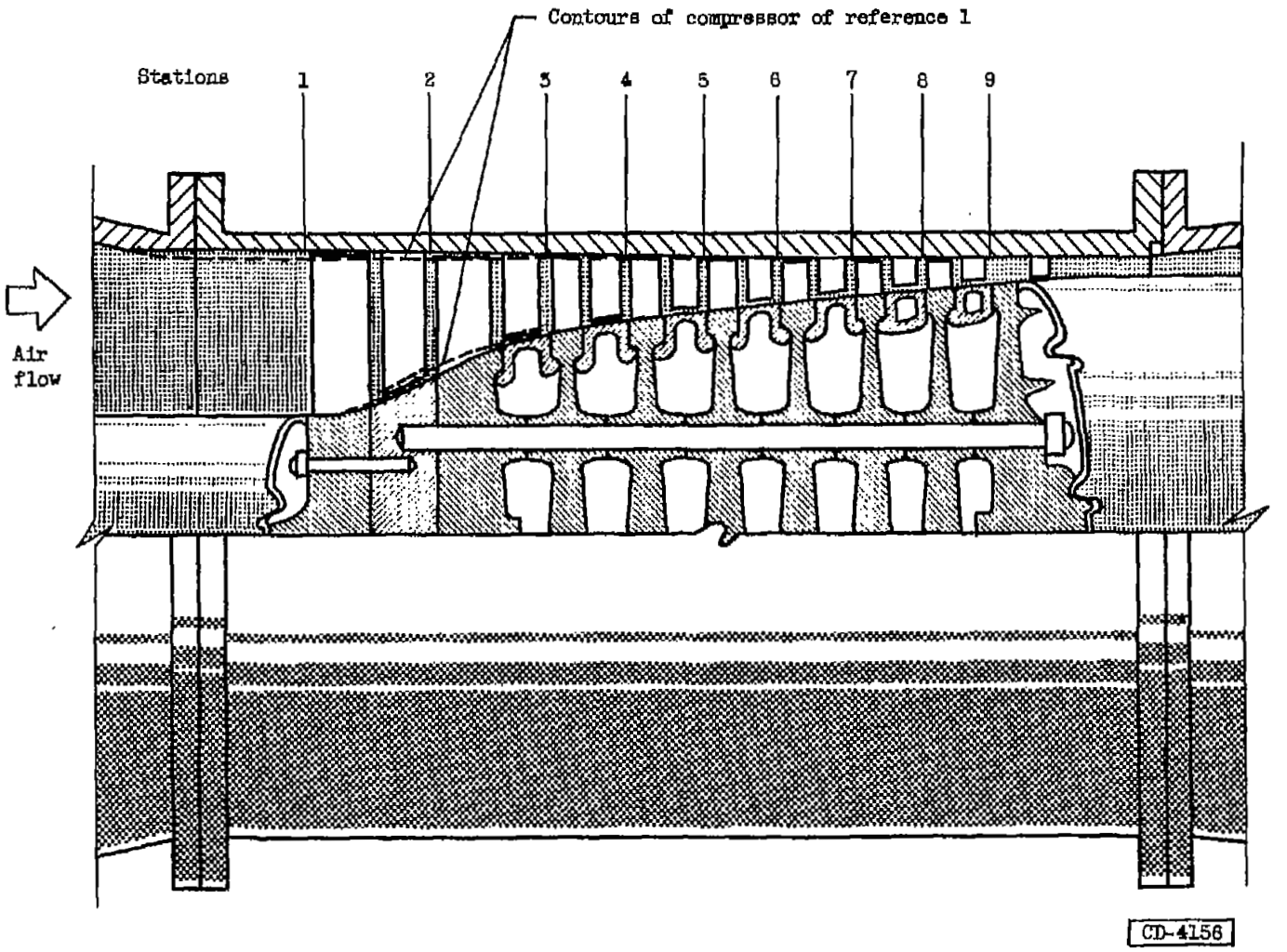


Figure 2. - Diagrammatic sketch of compressor flow passage and blading.

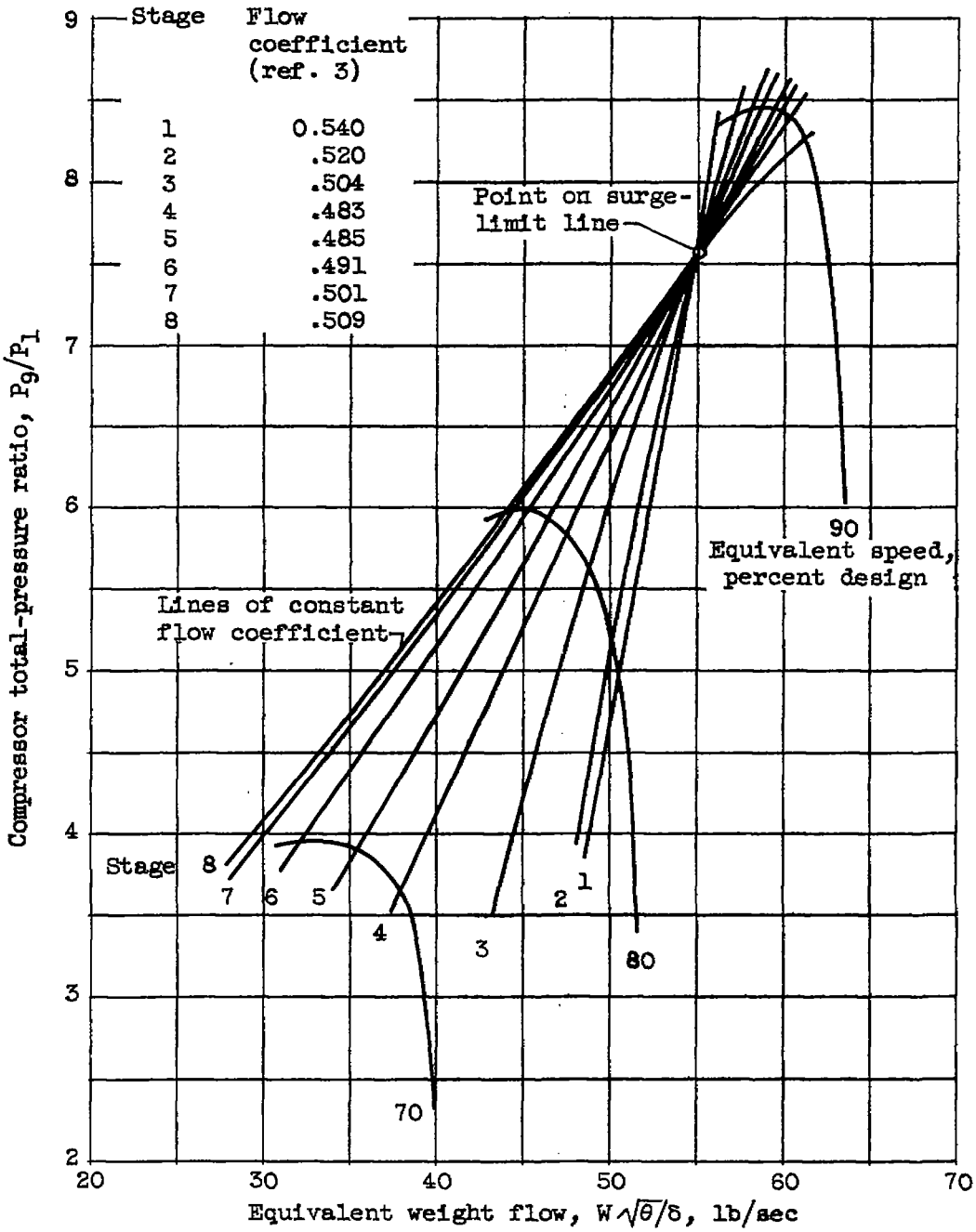


Figure 3. - Illustration of method used to approximate points on surge-limit line of modified eight-stage compressor.

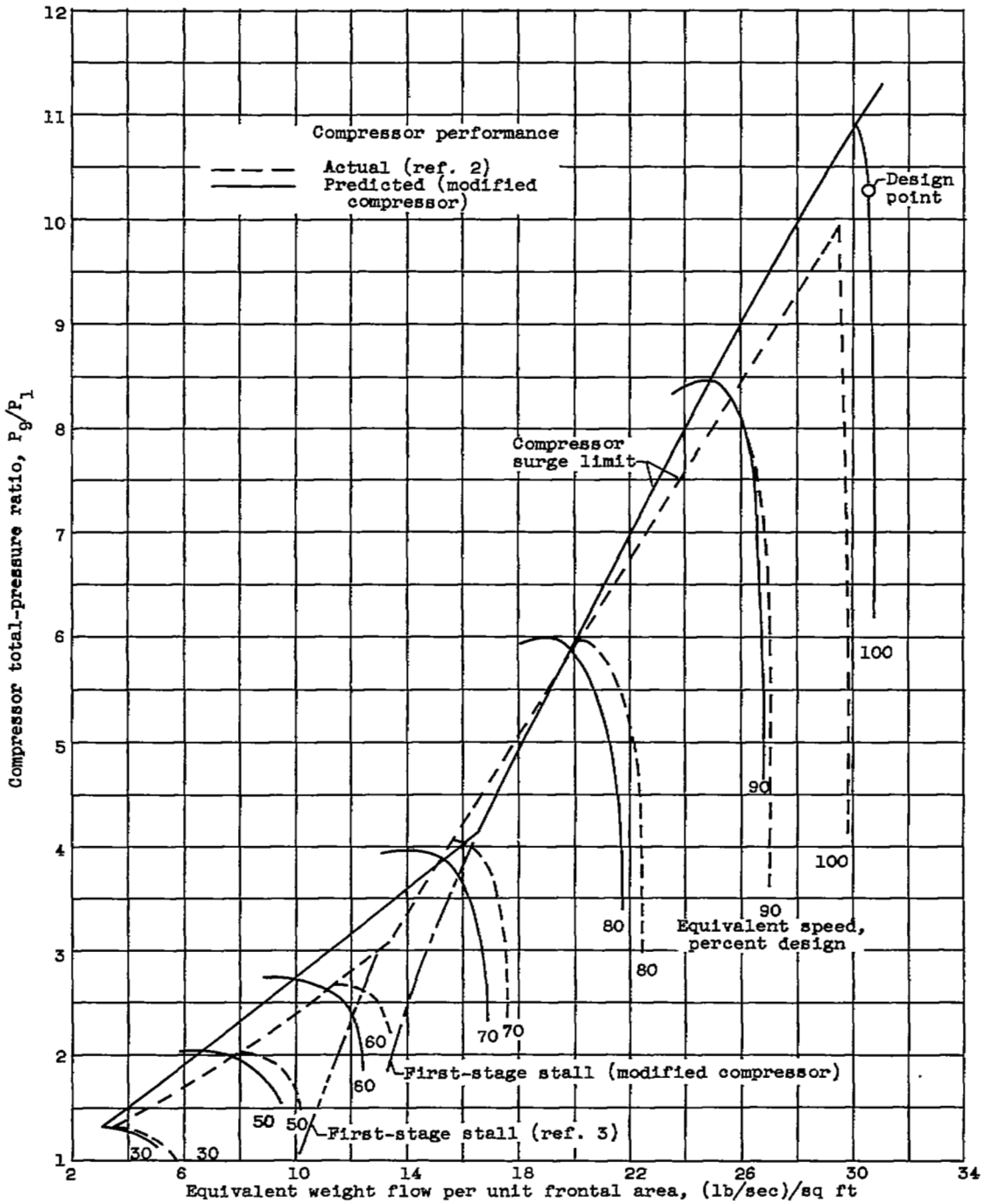


Figure 4. - Comparison of predicted performance of modified eight-stage compressor with actual performance of unmodified compressor.

[redacted]

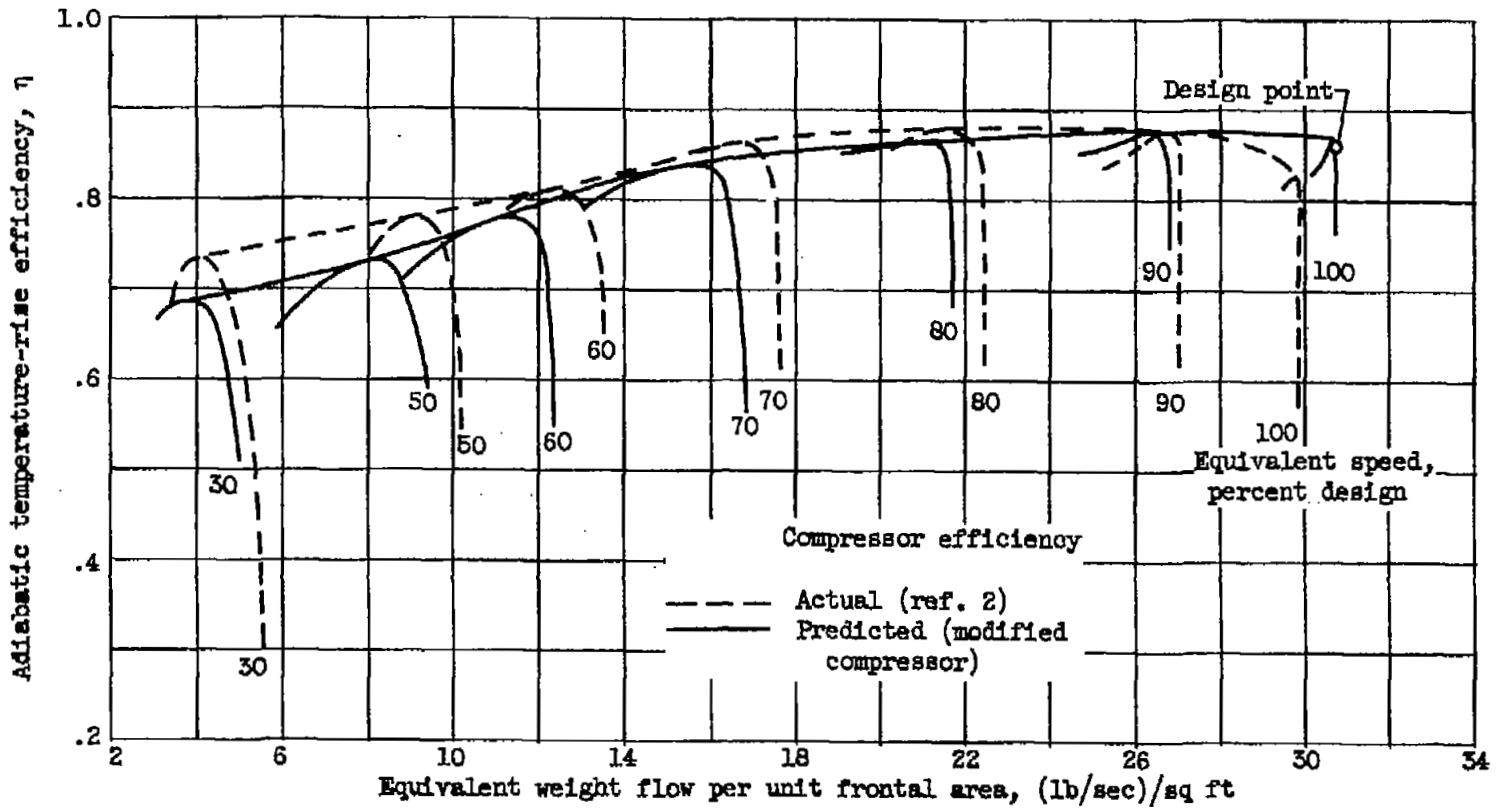


Figure 5. - Comparison of predicted efficiency of modified eight-stage compressor with actual efficiency of unmodified compressor.